THE JOURNAL OF PHYSICAL CHEMISTRY Letters

Letter

pubs.acs.org/JPCL

Improved Sensitivity for Long-Distance Measurements in Biomolecules: Five-Pulse Double Electron−Electron Resonance

Peter P. Borbat,* Elka R. Georgieva, and Jack H. Freed*

Department of Chemistry and Chemical Biology, Cornell University, Ithaca, New York 14853, United States

Supporting Information

ABSTRACT: We describe significantly improved long-distance measurements in biomolecules by use of the new multipulse double electron−electron spin resonance (DEER) illustrated with the example of a five-pulse DEER sequence. In this sequence, an extra pulse at the pump frequency is used compared with standard four-pulse DEER. The position of the extra pulse is fixed relative to the three pulses of the detection sequence. This significantly reduces the effect of nuclear spin-diffusion on the electron-spin phase relaxation, thereby enabling longer dipolar evolution times that are required to measure longer distances. Using spin-labeled T4 lysozyme at a concentration less than 50 μM, as an example, we show that the evolution time increases by a factor of 1.8 in protonated solution and 1.4 in deuterated solution to 8 and 12 μs, respectively, with the potential to increase them further. This enables a significant increase in the measurable distances, improved distance resolution, or both.

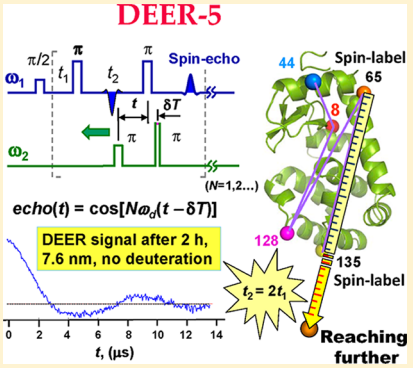

SECTION: Biophysical Chemistry and Biomolecules

Pulsed dipolar ESR spectroscopy (PDS), represented by double-electron electron resonance (DEER or PELDOR)[1] and double-quantum coherence electron spin resonance (DQC ESR),[2−6] has been developed into a versatile biophysical method of studying structure and function of biomolecules[5−10] on the nanoscale, (typically 1−9 nm) by measuring the strength of the electron spin dipole−dipole interaction between paramagnetic centers (tags). This enables the study of a variety of systems including membrane proteins,[11−13] large multiunit protein complexes;[14,15] proteins that undergo structural transformations,[16] and oligonucleotides and their complexes with proteins.[17,18] It is also being applied to study colloids and polymers,[19] supramolecular constructs,[20] and other nano-objects.[21,22] The electron spins are those of paramagnetic tags, usually nitroxide labels but also metal ions,[23] selectively introduced into desired positions of the biomolecule, although structural information has also been obtained by measuring distances between endogenous paramagnetic centers in proteins.[11,24−27]

Even though PDS technology has enjoyed an explosive growth, there are sensitivity issues because typical measurements usually can take ∼12 h and still do not provide sufficient SNR or distance resolution. Thus,[14,28−30] the need for improved efficiency is great, especially in the case of long distances of 5 nm or more. An order of magnitude improvement in concentration sensitivity has been achieved by conducting the experiment using spectrometers with high-power sources operating at Ku band or higher,[31−33] but the intrinsic properties of the sample contribute another problem. The PDS experiment is typically performed on frozen glassy solutions in the temperature range of 10 to 80 K to maximize SNR by optimizing spin−lattice relaxation time, T_1, and phase memory time, T_m, for various spin tags, with T_m being the major factor limiting the sensitivity and the range of distances that can be measured.[3] The main source of phase relaxation in most cases is echo dephasing caused by the fluctuating hyperfine coupling to the surrounding protons of the solvent and the biomolecule.[6,7,34,35] In spin-labeled proteins, buried residues usually have a T_m in the range of 0.6 to 2.0 μs, and relaxation is by a simple exponential decay, $\exp(-2t/T_m)$, (so that $T_m = T_2$ in this case), mainly due to protons of rotating methyl groups in the protein and the alkyl chains of lipids in membranes.[35,36] Spin labels attached to solvent-exposed residues have somewhat longer T_m values of about 2 to 3 μs because their relaxation for $t \gtrsim 2$ μs is dominated by nuclear spin diffusion in the protonated solvent, which contributes a temperature-independent relaxation decay $\exp[-(2t/T_m)^\kappa]$, with $\kappa \cong 1.5-3.5$; the value of 2 being typical.[37] In H_2O, T_m is ∼4 μs; therefore, the maximum evolution time, t (t_{max}), cannot be significantly greater than ∼5 μs even for the most sensitive DEER spectrometers available today. For 1.75 periods of dipolar oscillation (T_d) required for accurate distance analysis,[7] the maximum T_d corresponds to 4.5 to 5.5 nm. Somewhat less accurate measurements using $t_{max} \approx 1.25T_d$ can be used to estimate distances up to 5 to 6 nm. Any further improvement in accessible distances necessitates reducing the effect of nuclear spin diffusion, which for exposed residues is typically accomplished by using a deuterated solvent when possible. However just solvent deuteration rarely permits t_{max}

Received: November 4, 2012
Accepted: December 19, 2012
Published: December 19, 2012

exceeding 7 to 8 μs[38−42] because there are protons of the biomolecule itself. Ultimately, the protein can be deuterated in some cases,[39,40] but this is a costly and laborious solution, which may not always be practical or feasible for eukaryotic proteins or other cases.[43,44]

The current level of sensitivity (see, for example, Figure S1 in the Supporting Information (SI)) helps one to measure distances <5 nm more efficiently (Figure 2 and Figure S6 in the SI), which is important for spin tags in a hydrophobic environment, but only a very small improvement can be obtained beyond ∼3 μs for longer distances, where the exponent in t becomes quadratic or greater. A well-known solution to this problem is to minimize such relaxation by applying a pulse sequence that periodically refocuses the transverse magnetization.[45] For a sequence of n equally spaced (by 2τ) refocusing pulses, the echo decays by $\exp[-n(2\tau/nT_m)^\kappa] = \exp[-(2\tau/T_{eff})^\kappa]$, where the effective T_m becomes $T_{eff} = T_m n^{(1-1/\kappa)}$. For n and κ equal 2, this gives a factor of $2^{1/2}$ increase in T_m, but it doubles if n is 4.

Here we describe how such a multipulse approach is implemented in PDS, illustrating this with the example of a novel five-pulse DEER sequence, which allows the expansion of t_{max} with or without using deuterated solvent, thereby enabling accurate measurement of distances up to ∼8 to 9 nm. It can be used as a basic building block for prospective multipulse sequences realizing $n > 1$, as shown in the SI.

The standard four-pulse DEER sequence $\pi/2{-}t_1{-}\pi{-}t_2{-}\pi{-}(t_2{-}t_1){-}echo$, shown in Figure 1a, uses two refocusing pulses at the detection frequency ω_1; therefore, it has the potential to increase T_m as described above if $t_2 = 2t_1$. The modulation of the echo amplitude $V(t)$, due to the electron spin dipole−dipole coupling (or the "dipolar signal" for short), is produced by the "pump" π-pulse, applied at the frequency ω_2, by varying its position, t, between the two π-pulses at the detection frequency, yielding $V(t) = \cos[A(t - t_1)]$. Here $A = \omega_d(1 - 3\cos^2\theta)$, with $\omega_d = \mu_0\gamma_e^2\hbar/4\pi r^3$ being the line splitting produced by the static dipolar interaction between the two electron spins separated by distance, r, and θ being the angle between $\mathbf{r}$ and the external magnetic field. We assumed the weak coupling regime: $\omega_d \ll |\omega_1 - \omega_2|$, which is appropriate for the description of DEER or for long distances in general.[3,10] Averaging $V(t)$ over all orientations in A (represented by angular brackets) leads to decaying oscillations according to $V_4(t) = \langle\cos[A(t - t_1)]\rangle_A$ (Figure 1a, green curve) with a maximum at $t = t_1$, at which time the dipolar coupling is "refocused"; that is, the cosine has zero argument for all A. The maximum time interval available for recording $V_4(t)$ is $(t_2 - t_1)$, which is close to t_2 in a typical experiment in which one sets $t_2 \gg t_1$ to maximize the range of t, over which the dipolar evolution is obtained. The relaxation decay $R(t)$ of the echo in this pulse sequence due to nuclear spin diffusion is $R(t) = \exp[-(2t_1/T_m)^\kappa - (2(t_2 - t_1)/T_m)^\kappa]$. Thus in the typical implementation $t_2 \gg t_1$ and $R(t) \approx \exp[-(2t_2/T_m)^\kappa]$.

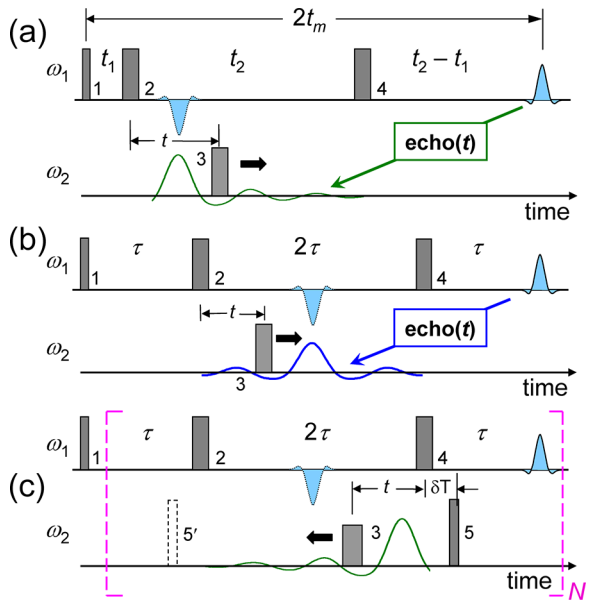

Figure 1. (a) Standard four-pulse DEER sequence with the respective dipolar modulation pattern plotted in green. (b) The four-pulse sequence modified for $t_2 = 2t_1 \equiv 2\tau$ to minimize nuclear spin diffusion, thus, increasing the signal, but this shifts the dipolar modulation (in blue) to the middle of the second interval, thereby losing half of the dipolar modulation because the halves are identical. (c) Placing the second pump pulse, 5, after the pulse 4 shifts dipolar modulation toward pulse 4, thereby recovering the full time span, 2τ. The dipolar modulation (green) is reversed in time compared with panel a. Pulse 5 could also be placed at position 5′ before pulse 2, reversing the modulated time trace. Note that time period, t_m, available for recording the dipolar signal is (a) t_2 and (b,c) 2τ.

In the case of $t_2 = 2t_1$, the maximum is in the middle of the second interval (Figure 1b), and only half of the time trace can be recorded. This more than offsets the gain that could be achieved by "stretching" the sequence in panel b by a factor of $\sim 2^{1/2}$ enabled by the longer T_m compared with the sequence in panel a. This situation, however, is remedied by adding to the sequence b an additional π pulse at ω_2 placed at a fixed position right after pulse 4. The pulse is denoted as 5 in Figure 1c. The dipolar signal is recorded in a manner similar to panel b by varying the position of pulse 3 to span the same interval between detection pulses 2 and 4. The time interval t_2 is again set to $2t_1$ to minimize the phase relaxation caused by the nuclear spin diffusion by refocusing the primary echo exactly in the middle of the interval of $2t_m$ made by the first $\pi/2$ pulse and the refocused primary echo, (i.e., at t_m). This new five-pulse DEER sequence (DEER-5) however, utilizes for the dipolar evolution all the time from the first pulse to the spin echo, enabling its expansion to longer t_m (half the distance from pulse 1 to the refocused echo for all three pulse sequences shown). The dipolar modulation is given by $V_5(t) = \langle\cos[A(t - \delta T)]\rangle_A$, where $\delta T \approx 50{-}100$ ns to ensure zero dead-time. The derivation of this result can be found in the SI, and its discussion appears later in the text. The four-pulse block of the sequence enclosed in red brackets can be repeated to provide a train of $n = 2N$ refocusing pulses at ω_1, as does the Carr−Purcell (CP) sequence,[45] but it also has $2N$ pump pulses at ω_2, with the position of every other pulse fixed and the rest spanning their respective intervals, exactly as does the first block. This results in the principal dipolar signal with the form $V_5(t) = \langle\cos[AN(t{-}\delta T)]\rangle_A$ (see SI). The present study has its focus on the case $N = 1$ ($n = 2$), that is, just the basic five-pulse DEER, but two- or three-frame sequences ($N = 2,3$), with n equals 4 or 6, may also be practical (see SI). The main distinction from a CP or CPMG (Carr−Purcell−Meiboom−Gill[46]) sequence is that this sequence is designed for measuring the dipolar interaction.

Because the echo relaxation decay is a function of t_m and the positions of refocusing pulses at ω_1 (cf. Figure 1), Figure 2 compares the standard DEER-4 (Figure 1a) to DEER-5 (Figure

dx.doi.org/10.1021/jz301788n | J. Phys. Chem. Lett. 2013, 4, 170−175

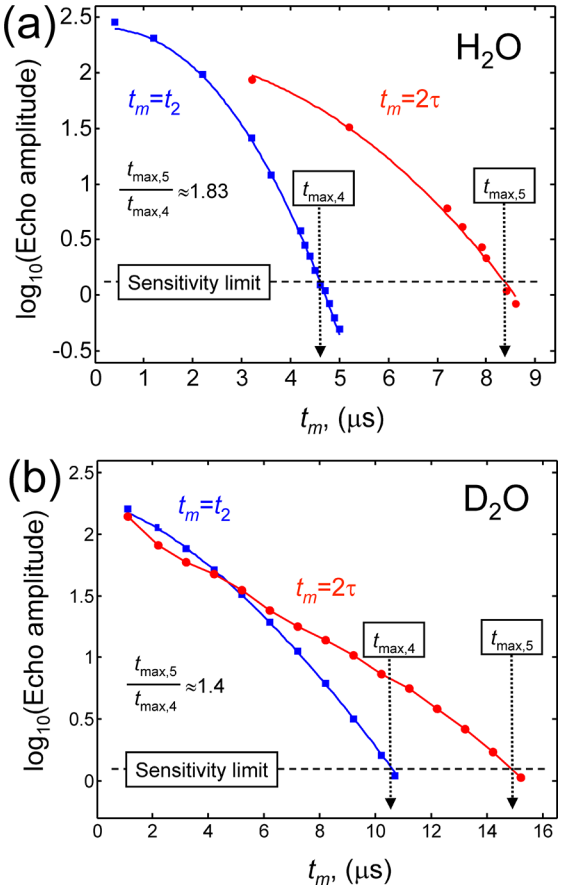

Figure 2. Comparison of the echo amplitude for the same sample of 40 μM T4L 8/44, recorded as a function of dipolar evolution time period, t_m, with standard four-pulse DEER (in blue) and five-pulse DEER (in red) (cf. Figure 1). The five-pulse DEER signal decays much slower as the pulse sequence expands in time, leading to an increase in the time period, t_{max}, available for recording the dipolar signal factor by the factor of 1.83 for H_2O (a) and 1.4 for D_2O (b). The echo amplitude shown is in mV and is the receiver output for constant gain.

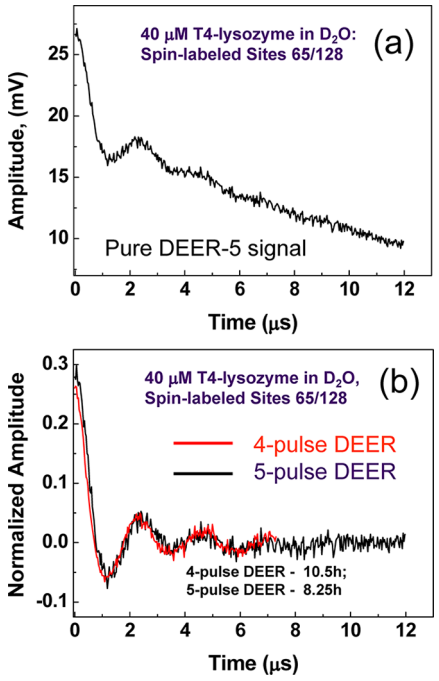

Figure 3. (a) DEER-5 signal recorded in D_2O buffer is shown after subtracting the residual unwanted DEER-4 type dipolar signal. (b) After standard baseline removal, the DEER-5 data (in black) are plotted together with standard four-pulse DEER data (in red), normalized according to the literature.[41]

1c) by plotting the spin−echo amplitude as a function of t_m for the T4-lysozyme (T4L) mutant spin-labeled at sites 8 and 44 and prepared in 40 μM concentration in H_2O and D_2O buffers with 30% (w/v) glycerol or glycerol-d_8. The data were taken at 17.3 GHz and 60 K. The maximum time in t_m, t_{max}, was expanded by a factor of ~1.83 in H_2O, whereas only a factor of 1.52, corresponding to $\kappa \approx 2.5$ determined for this sample, was expected.[47] The maximum time is taken at the point in t_m where the spin−echo drops to the "sensitivity threshold" level, which is defined as corresponding to a SNR ~10 in the modulated part of the complete DEER record after ~3 h of data averaging. Because the echo amplitude at the threshold (horizontal dashed line) is only ~0.003 of its value for $t_m < 1$ μs for the H_2O sample (equivalent to a ~0.2 μM protein with $T_m = \infty$), this is the "hard limit".

We next show in Figure 3a the result from the DEER-5 experiment conducted under the same conditions but with a sample of T4-lysozyme with MTS spin labels incorporated at positions 65 and 128 and prepared in D_2O buffer containing 30% w/v glycerol-d_8. In Figure 3b, this signal is shown after standard DEER baseline subtraction together with the data obtained on this sample using the standard DEER-4. In this case, standard DEER-4 can be recorded to very good SNR up to ~7 to 8 μs,[41] whereas DEER-5 was recorded on a 12 μs time scale, which allows distances up to 8 nm to be reliably determined using just matrix deuteration. We do show in the SI measurements of 8 nm in a fully protonated system (cf. Figure S6 in the Supporting Information). (Note that the DEER-5 signal in Figure 3a was preprocessed to remove the residual unwanted dipolar signal, as explained later in the text).

We describe the issues underlying the pulse method developed in this work, including the details of dipolar evolution and the respective signals in a multipulse sequence in the SI. Here we simply note that when more than one π-pulse is applied at the pump frequency the situation leads to more than one dipolar signal and they generally have different time dependences. Because in DEER each π-pulse is selective, it changes the direction of the dipolar evolution for some spins at ω_2, thus branching the dipolar evolution into two "dipolar pathways", that is, those that are flipped and those that are not. For n pump π-pulses there are 2^n pathways. They generally have different time variables and sets of refocusing points. Five-pulse DEER thus has four dipolar pathways. The probability (weight), w_k, of a given pathway is a product of n terms, s_k, with s_k either p_k or q_k, which are the probabilities, p_k, for pump pulse k to flip the spin or have no effect, q_k (where $q_k = 1 - p_k$).

On the basis of an analysis of possible dipolar pathways in DEER-5 (see SI), we can write for the intramolecular part of the dipolar signal in five-pulse DEER

$$V_{intra}(t) \propto \langle q_3 q_5 + q_3 p_5 \cos[A(\tau - \delta T)] + p_3 q_5 \cos[A(t - \tau)] + p_3 p_5 \cos[A(t - \delta T)] \rangle_{orientations} \quad (1)$$

The first and the second terms in eq 1 are constant in t, so they just contribute a background ~$q_3 q_5$; the third term is the

dx.doi.org/10.1021/jz301788n | J. Phys. Chem. Lett. 2013, 4, 170−175

unwanted residual of the DEER-4 dipolar signal that exists in the absence of the fifth pulse. It is present when $\langle p_3 q_5 \rangle \neq 0$. The fourth term gives the new DEER-5 specific dipolar signal. The angular brackets denote averaging over all orientations and Euler angles for all magnetic tensors. The smaller $\langle p_3 q_5 \rangle$, the better the suppression of the unwanted signal.

On the basis of eq 1, the intermolecular contribution to the signal can be derived to be (see SI)

$$V_{\text{inter}}(t) \propto \exp[\langle -k_0 C(q_3 p_5 |\tau - \delta T| + p_3 q_5 |t - \tau| + p_3 p_5 |t - \delta T|)\rangle_{\omega_2}] \quad (2)$$

Here C is the concentration of spins, $k_0 = 2\pi\mu_0\gamma_e^2\hbar/9{\cdot}3^{1/2} \approx 0.972 \times 10^{-3}\ \mu\text{M}^{-1}\ \mu\text{s}^{-1}$. The angular brackets denote integration over the ESR spectrum because there is no orientational correlation with randomly distributed surrounding spins. The signal $V(t)$ becomes a product $V(t) = V_{\text{intra}}(t) V_{\text{inter}}(t)$. The eqs 1 and 2 describe the appearance of the raw data in Figure 4a and in the SI.

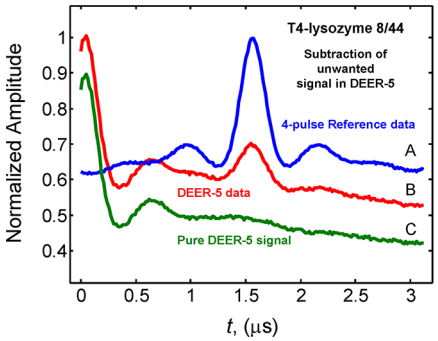

Figure 4. Isolation of pure DEER-5 signal. The reference, A, was recorded in the absence of the fifth pulse and used in the removal of the incompletely suppressed dipolar signal of A-type from the raw signal, B, recorded in the presence of the fifth pulse. C indicates the pure five-pulse dipolar signal produced by subtracting scaled down A from B. A–C are normalized to unit amplitude at their maxima, with C shifted by −0.1 for clarity.

Because not all spins flipped by pulse 3 are also flipped by pulse 5, that is, $q_5 \neq 0$ for some $p_3 \neq 0$, the term $\langle p_3 q_5 \cos[A(t - \tau)]\rangle$ in eq 1 is nonzero, so this incompletely suppressed signal coexists with the dominant term $\langle p_3 p_5 \cos[A(t - \delta T)]\rangle$ representing the pure DEER-5 specific signal. It appears as a central hump in the raw signal time trace, recorded with the five-pulse sequence, although it is significantly attenuated when a more nonselective higher intensity pulse 5 is applied. Both signals share the same coherence pathway and cannot be separated by phase cycling. This undesired signal can be nearly entirely suppressed by achieving the condition $q_5 = 0$ (or $p_5 = 1$) for all spectral points where $p_3 \neq 0$; that is, this pulse should provide uniform selective population inversion, and pulse 3 does not affect spins outside this uniformly inverted region. It was approximated in this work by setting pulse 5 to be more intense (12 ns width) than pulse 3 (26–29 ns width), thereby suppressing the four-pulse signal by a factor of 3 to 6 (cf. Figures 3 and 4c and the SI). The residual unwanted signal is further reduced by subtracting out the scaled down pure four-pulse reference signal recorded with pulse 5 turned off. (This does not noticeably increase data recording time or degrade SNR if the unwanted modulation is a small fraction of the reference modulation). The subtraction is illustrated in Figure 3, with more examples shown in the SI. Taken together, these two steps suppress the unwanted signal by a factor of ∼20 or more, which is down to the typical level of artifacts and distortions in DEER or DQC.

There is clearly room for improvement, as discussed in the SI. Ultimately, pulse 5 should be shaped (cf. SI Figure S4 for preliminary experiments) to provide more uniform population inversion and at the same time to compensate for moderate B_1 inhomogeneity,[48,49] thereby simplifying the experiment by making the referencing easier or removing the need for it.

The novel five-pulse DEER method introduced in this work has considerable potential to develop into a widely useful technique to study nanoscale systems, wherein long or more accurate distances need to be measured, but also it could help to considerably shorten data measurements by offering greater sensitivity than could be achieved using standard DEER methods. It can be easily implemented with any modern spectrometer in its current form. Whereas our data are shown for a working frequency in the Ku band, similar relative gains are expected for other frequencies as well, but in each case, the longest distance that could be measured will be dependent on the concentration sensitivity of the spectrometer. By further technical development, enabled by modern technology permitting generation of high-speed complex pulse modulation schemes at mw- and mm-wave frequencies, the method is expected to be improved and find wide use in PDS, adding to the established PDS methods of DQC-ESR and DEER. It may become an enabling technology, for example, to study eukaryotic proteins and also materials, where, for example, matrix or solute deuteration is impractical or not feasible.

EXPERIMENTAL METHODS

The experiments were conducted on nitroxide-labeled T4L double mutants using the ACERT Ku-band (17.3 GHz) PDS spectrometer (both DEER and DQC). All T4L mutants used in this study were previously well-characterized by standard four-pulse DEER.[41] Further experimental details and sample preparation protocols are included in the SI.

ASSOCIATED CONTENT

Supporting Information

(1) Experimental details; (2) analysis of dipolar pulse sequences; (3) intermolecular effects; (4) data processing; (5) examples; and (6) comparison of PDS methods. This information is available free of charge via the Internet at http://pubs.acs.org/.

AUTHOR INFORMATION

Corresponding Author

*E-mail: ppb@ccmr.cornell.edu; Tel: (607) 255-6132; Fax: (607) 255-6969 (P.P.B.). E-mail: jhf3@cornell.edu; Tel: (607) 255-3647; Fax: (607) 255-6969 (J.H.F.)

Notes

The authors declare no competing financial interest.

ACKNOWLEDGMENTS

We thank Dr. Cynthia Kinsland for advising on the mutagenesis. AddGene is acknowledged for the plasmid #18111 encoding cysteine-less wild-type T4-Lysozyme, developed in the laboratory of Prof. Brian Matthews. T4L mutants were expressed at the Protein Facility of Cornell University. We are grateful to Dr. Gunnar Jeschke for kindly providing samples

of long biradicals and to Drs. Murali Krishna, Sankaran Subramanian, Nallathamby Devasahayam, and Kevin Hobbs for their help with the spectrometer software. This work was supported by grants NIH/NCRR P41-RR 016292, NIH/NIGMS P41GM103521, and NIH/NIBIB R010EB003150. A preliminary account of this work (five-pulse DEER) was presented at the 54th Rocky Mountain Conference on Analytical Chemistry, July 15−19, 2012, Copper Conference Center, Copper Mountain, Colorado. Peter Borbat, Elka R. Georgieva, and Jack H. Freed, Pulsed Dipolar ESR Spectroscopy with Improved Sensitivity.

REFERENCES

(1) Pannier, M.; Veit, S.; Godt, A.; Jeschke, G.; Spiess, H. W. Dead-Time Free Measurement of Dipole-Dipole Interactions between Electron Spins. *J. Magn. Reson.* **2000**, *142*, 331−40.

(2) Borbat, P. P.; Freed, J. H. ESR Multiple-Quantum and Distance Measurements. *Chem. Phys. Lett.* **1999**, *313*, 145−154.

(3) Borbat, P. P.; Freed, J. H. ESR Double-Quantum and Distance Measurements. In *Biological Magnetic Resonance*; Berliner, L. J., Eaton, S. S., Eaton, G. R., Eds.; Kluwer Academics/Plenum Publishers: New York, 2000; Vol. *19*, pp 383−459.

(4) Fafarman, A. T.; Borbat, P. P.; Freed, J. H.; Kirshenbaum, K. Characterizing the Structure and Dynamics of Folded Oligomers: Pulsed ESR Studies of Peptoid Helices. *Chem. Commun.* **2007**, 377−379.

(5) Borbat, P. P.; Freed, J. H. Pros and Cons of Pulse Dipolar ESR: DQC and DEER. *EPR Newsletter* **2007**, *17*, 21−33.

(6) Borbat, P. P.; Freed, J. H. Measuring Distances by Pulsed Dipolar ESR Spectroscopy: Spin-Labeled Histidine Kinases. *Methods Enzymol.* **2007**, *423*, 52−116.

(7) Jeschke, G.; Polyhach, Y. Distance Measurements on Spin-Labelled Biomacromolecules by Pulsed Electron Paramagnetic Resonance. *Phys. Chem. Chem. Phys.* **2007**, *9*, 1895−1910.

(8) Schiemann, O.; Prisner, T. F. Long-Range Distance Determinations In Biomacromolecules By EPR Spectroscopy. *Q. Rev. Biophys.* **2007**, *40*, 1−53.

(9) Reginsson, G. W.; Schiemann, O. Pulsed Electron-Electron Double Resonance: Beyond Nanometre Distance Measurements on Biomacromolecules. *Biochem. J.* **2011**, *434*, 353−363.

(10) Milov, A. D.; Maryasov, A. G.; Tsvetkov, Y. D. Pulsed Electron Double Resonance (PELDOR) and its Aplications in Free-Radical Research. *Appl. Magn. Reson.* **1998**, *15*, 107−143.

(11) Upadhyay, A. K.; Borbat, P. P.; Wang, J.; Freed, J. H.; Edmondson, D. E. Determination of the Oligomeric States of Human and Rat Monoamine Oxidases in The Outer Mitochondrial Membrane and Octyl Beta-D-Glucopyranoside Micelles Using Pulsed Dipolar Electron Spin Resonance Spectroscopy. *Biochemistry* **2008**, *47*, 1554−1566.

(12) Smirnova, I.; Kasho, V.; Choe, J. Y.; Altenbach, C.; Hubbell, W. L.; Kaback, H. R. Sugar Binding Induces an Outward-Facing Conformation of LacY. *Proc. Natl. Acad. Sci. U. S. A.* **2007**, *104*, 16504−16509.

(13) Mchaourab, H. S.; Steed, P. R.; Kazmier, K. Toward the Fourth Dimension of Membrane Protein Structure: Insight into Dynamics from Spin-Labeling EPR Spectroscopy. *Structure* **2011**, *19*, 1549−1561.

(14) Bhatnagar, J.; Borbat, P. P.; Pollard, A. M.; Bilwes, A. M.; Freed, J. H.; Crane, B. R. Structure of the Ternary Complex Formed by a Chemotaxis Receptor Signaling Domain, the CheA Histidine Kinase, and the Coupling Protein CheW As Determined by Pulsed Dipolar ESR Spectroscopy. *Biochemistry* **2010**, *49*, 3824−3841.

(15) Grote, M.; Polyhach, Y.; Jeschke, G.; Steinhoff, H. J.; Schneider, E.; Bordignon, E. Transmembrane Signaling in the Maltose ABC Transporter MalFGK(2)-E Periplasmic MalF-P2 Loop Communicates Substrate Availability to the ATP-Bound MalK Dimer. *J. Biol. Chem.* **2009**, *284*, 17521−17526.

(16) Van Eps, N.; Preininger, A. M.; Alexander, N.; Kaya, A. I.; Meier, S.; Meiler, J.; Hamm, H. E.; Hubbell, W. L. Interaction of a G Protein with an Activated Receptor Opens the Interdomain Interface in the Alpha Subunit. *Proc. Natl. Acad. Sci. U. S. A.* **2011**, *108*, 9420−9424.

(17) Wunnicke, D.; Ding, P.; Seela, F.; Steinhoff, H. J. Site-Directed Spin Labeling of DNA Reveals Mismatch-Induced Nanometer Distance Changes between Flanking Nucleotides. *J. Phys. Chem. B* **2012**, *116*, 4118−4123.

(18) Butala, M.; Klose, D.; Hodnik, V.; Rems, A.; Podlesek, Z.; Klare, J. P.; Anderluh, G.; Busby, S. J. W.; Steinhoff, H. J.; Zgur-Bertok, D. Interconversion between bound and free conformations of LexA Orchestrates the Bacterial SOS Response. *Nucleic Acids Res.* **2011**, *39*, 6546−6557.

(19) Ruthstein, S.; Potapov, A.; Raitsimring, A. M.; Goldfarb, D. Double Electron Electron Resonance as a Method for Characterization of Micelles. *J. Phys. Chem. B* **2005**, *109*, 22843−22851.

(20) Lovett, J. E.; Hoffmann, M.; Cnossen, A.; Shutter, A. T. J.; Hogben, H. J.; Warren, J. E.; Pascu, S. I.; Kay, C. W. M.; Timmel, C. R.; Anderson, H. L. Probing Flexibility in Porphyrin-Based Molecular Wires Using Double Electron Electron Resonance. *J. Am. Chem. Soc.* **2009**, *131*, 13852−13859.

(21) Gulla, S. V.; Sharma, G.; Borbat, P.; Freed, J. H.; Ghimire, H.; Benedikt, M. R.; Holt, N. L.; Lorigan, G. A.; Rege, K.; Mavroidis, C.; Budil, D. E. Molecular-Scale Force Measurement in a Coiled-Coil Peptide Dimer by Electron Spin Resonance. *J. Am. Chem. Soc.* **2009**, *131*, 5374−5375.

(22) Kurzbach, D.; Kattnig, D. R.; Zhang, B. Z.; Schluter, A. D.; Hinderberger, D. Assessing the Solution Shape and Size of Charged Dendronized Polymers Using Double Electron-Electron Resonance. *J. Phys. Chem. Lett.* **2011**, *2*, 1583−1587.

(23) Yagi, H.; Banerjee, D.; Graham, B.; Huber, T.; Goldfarb, D.; Otting, G. Gadolinium Tagging for High-Precision Measurements of 6 nm Distances in Protein Assemblies by EPR. *J. Am. Chem. Soc.* **2011**, *133*, 10418−10421.

(24) Kay, C. W.; Elsasser, C.; Bittl, R.; Farrell, S. R.; Thorpe, C. Determination of The Distance between the Two Neutral Flavin Radicals in Augmenter of Liver Regeneration by Pulsed ELDOR. *J. Am. Chem. Soc.* **2006**, *128*, 76−77.

(25) Bennati, M.; Robblee, J. H.; Mugnaini, V.; Stubbe, J.; Freed, J. H.; Borbat, P. EPR Distance Measurements Support a Model for Long-Range Radical Initiation in E. Coli Ribonucleotide Reductase. *J. Am. Chem. Soc.* **2005**, *127*, 15014−15015.

(26) Yang, Z. Y.; Kurpiewski, M. R.; Ji, M.; Townsend, J. E.; Mehta, P.; Jen-Jacobson, L.; Saxena, S. ESR Spectroscopy Identifies Inhibitory Cu2+ Sites in a DNA-modifying Enzyme to Reveal Determinants of Catalytic Specificity. *Proc. Natl. Acad. Sci. U. S. A.* **2012**, *109*, E993−E1000.

(27) Astashkin, A. V.; Rajapakshe, A.; Cornelison, M. J.; Johnson-Winters, K.; Enemark, J. H. Determination of the Distance between the Mo(V) and Fe(III) Heme Centers of Wild Type Human Sulfite Oxidase by Pulsed EPR Spectroscopy. *J. Phys. Chem. B* **2012**, *116*, 1942−1950.

(28) Park, S.-Y.; Borbat, P. P.; Gonzalez-Bonet, G.; Bhatnagar, J.; Pollard, A. M.; Freed, J. H.; Bilwes, A. M.; Crane, B. R. Reconstruction of the Chemotaxis Receptor-Kinase Assembly. *Nat. Struct. Mol. Biol.* **2006**, *13*, 400−407.

(29) Zou, P.; Bortolus, M.; Mchaourab, H. S. Conformational Cycle of the ABC Transporter MsbA in Liposomes: Detailed Analysis Using Double Electron-Electron Resonance Spectroscopy. *J. Mol. Biol.* **2009**, *393*, 586−597.

(30) Grote, M.; Bordignon, E.; Polyhach, Y.; Jeschke, G.; Steinhoff, H. J.; Schneider, E. A Comparative Electron Paramagnetic Resonance Study of The Nucleotide-Binding Domains' Catalytic Cycle in the Assembled Maltose ATP-Binding Cassette Importer. *Biophys. J.* **2008**, *95*, 2924−2938.

(31) Polyhach, Y.; Bordignon, E.; Tschaggelar, R.; Gandra, S.; Godt, A.; Jeschke, G. High Sensitivity and Versatility of the DEER

Experiment on Nitroxide Radical Pairs at Q-Band Frequencies. *Phys. Chem. Chem. Phys.* **2012**, *14*, 10762−10773.
(32) Cruickshank, P. A. S.; Bolton, D. R.; Robertson, D. A.; Hunter, R. I.; Wylde, R. J.; Smith, G. M. A Kilowatt Pulsed 94 GHz Electron Paramagnetic Resonance Spectrometer with High Concentration Sensitivity, High Instantaneous Bandwidth, and Low Dead Time. *Rev. Sci. Instrum.* **2009**, *80*, 103102−103115.
(33) Borbat, P. P.; Crepeau, R. H.; Freed, J. H. Multifrequency Two-Dimensional Fourier Transform ESR: An X/Ku-Band Spectrometer. *J. Magn. Reson.* **1997**, *127*, 155−167.
(34) Milov, A. D.; Salikhov, K. M.; Tsvetkov, Y. D. Phase Relaxation of Hydrogen Atoms Stabilized in an Amorphous Matrix. *Phys. Solid State* **1973**, *15*, 802−806.
(35) Huber, M.; Lindgren, M.; Hammarstrom, P.; Martensson, L.-G.; Carlsson, U.; Eaton, G. R.; Eaton, S. S. Phase Memory Relaxation Times of Spin Labels in Human Carbonic Anhydrase II: Pulsed EPR to Determine Spin Label Location. *Biophys. Chem.* **2001**, *94*, 245−256.
(36) Lindgren, M.; Eaton, G. R.; Eaton, S. S.; Jonsson, B.-H.; Hammarstrom, P.; Svensson, M.; Carlsson, U. Electron Spin Echo Decay as a Probe of Aminoxyl Environment in Spin-Labeled Mutants of Human Carbonic Anhydrase II. *J. Chem. Soc., Perkin Trans.* **1997**, *2*, 2549−2554.
(37) Zecevic, A.; Eaton, G. R.; Eaton, S. S.; Lindgren, M. Dephasing of Electron Spin Echoes for Nitroxyl Radicals in Glassy Solvents by Non-Methyl and Methyl Protons. *Mol. Phys.* **1998**, *95*, 1255−1263.
(38) Georgieva, E. R.; Ramlall, T. F.; Borbat, P. P.; Freed, J. H.; Eliezer, D. Membrane-Bound Alpha-Synuclein Forms an Extended Helix: Long-Distance Pulsed ESR Measurements Using Vesicles, Bicelles, and Rodlike Micelles. *J. Am. Chem. Soc.* **2008**, *130*, 12856−12857.
(39) Georgieva, E. R.; Ramlall, T. F.; Borbat, P. P.; Freed, J. H.; Eliezer, D. The Lipid-Binding Domain of Wild Type and Mutant Alpha-Synuclein: Compactness and Interconversion between the Broken and Extended Helix Forms. *J. Biol. Chem.* **2010**, *285*, 28261−28274.
(40) Ward, R.; Bowman, A.; Sozudogru, E.; El-Mkami, H.; Owen-Hughes, T.; Norman, D. G. EPR Distance Measurements in Deuterated Proteins. *J. Magn. Reson.* **2010**, *207*, 164−167.
(41) Georgieva, E. R.; Roy, A. S.; Grigoryants, V. M.; Borbat, P. P.; Earle, K. A.; Scholes, C. P.; Freed, J. H. Effect of Freezing Conditions on Distances and Their Distributions Derived From Double Electron Electron Resonance (DEER): A Study of Doubly-Spin-Labeled T4 Lysozyme. *J. Magn. Reson.* **2012**, *216*, 69−77.
(42) Ward, R.; Bowman, A.; El-Mkami, H.; Owen-Hughes, T.; Norman, D. G. Long Distance PELDOR Measurements on the Histone Core Particle. *J. Am. Chem. Soc.* **2009**, *131*, 1348−1349.
(43) Katz, J. J.; Crespi, H. L. Deuterated organisms: cultivation and uses. *Science* **1966**, *151*, 1187−1194.
(44) Gardner, K. H.; Kay, L. E. The Use of 2H, 13C, 15N Multidimensional NMR to Study the Structure and Dynamics of Proteins. *Annu. Rev. Biophys. Biomol. Struct.* **1998**, *27*, 357−406.
(45) Carr, H. Y.; Purcell, E. M. Effects of Diffusion on Free Precession in Nuclear Magnetic Resonance Experiments. *Phys. Rev.* **1954**, *94*, 630−638.
(46) Meiboom, S.; Gill, D. Modified Spin-Echo Method for Measuring Nuclear Relaxation Times. *Rev. Sci. Instrum.* **1958**, *29*, 688−691.
(47) Borbat, P. P.; Davis, J. H.; Butcher, S. E.; Freed, J. H. Measurement of Large Distances in Biomolecules Using Double-Quantum Filtered Refocused Electron Spin-Echoes. *J. Am. Chem. Soc.* **2004**, *126*, 7746−7747.
(48) Warren, W. S. Effects of Arbitrary Laser or NMR Pulse Shapes on Population-Inversion and Coherence. *J. Chem. Phys.* **1984**, *81*, 5437−5448.
(49) Silver, M. S.; Joseph, R. I.; Hoult, D. I. Selective Spin Inversion in Nuclear Magnetic-Resonance and Coherent Optics Through an Exact Solution of The Bloch-Riccati Equation. *Phys. Rev. A* **1985**, *31*, 2753−2755.